

Remote His50 Acts as a Coordination Switch in the High-Affinity N-Terminal Centered Copper(II) Site of α -Synuclein

This is the peer reviewed version of the following article:

Original:

DE RICCO, R., Valensin, D., Dell'Acqua, S., Casella, L., Dorlet, P., Faller, P., et al. (2015). Remote His50 Acts as a Coordination Switch in the High-Affinity N-Terminal Centered Copper(II) Site of α -Synuclein. INORGANIC CHEMISTRY, 54(10), 4744-4751 [10.1021/acs.inorgchem.5b00120].

Availability:

This version is available <http://hdl.handle.net/11365/980594> since 2017-09-21T11:20:11Z

Published:

DOI: <http://doi.org/10.1021/acs.inorgchem.5b00120>

Terms of use:

Open Access

The terms and conditions for the reuse of this version of the manuscript are specified in the publishing policy. Works made available under a Creative Commons license can be used according to the terms and conditions of said license.

For all terms of use and more information see the publisher's website.

(Article begins on next page)

Remote His50 acts as a coordination switch in the high-affinity N-terminal centered copper(II) site of α -synuclein.

Riccardo De Ricco,^{a,b,c} Daniela Valensin,^{c,*} Simone Dell'Acqua,^d Luigi Casella,^d Pierre Dorlet,^e Peter Faller,^{a,b} Christelle Hureau,^{a,b,*}

^a CNRS, LCC (Laboratoire de Chimie de Coordination), 205 route de Narbonne, BP 44099, F-31077 Toulouse Cedex 4, France

^b Université de Toulouse, UPS, INPT, F-31077 Toulouse Cedex 4, France

^c Department of Biotechnology, Chemistry and Pharmacy, University of Siena, Via A. Moro 2, 53100 Siena, Italy.

^d Department of Chemistry, University of Pavia, Via Taramelli 12, 27100 Pavia, Italy

^e Institute for Integrative Biology of the Cell (I2BC), Laboratoire Stress Oxydant et Détoxication, CNRS UMR9198, Université Paris-Saclay, 91191 Gif sur Yvette Cedex, France

christelle.hureau@lcc-toulouse.fr, +33 5 61 33 31 62

daniela.valensin@unisi.it, +39 05 77 23 45 34

Abstract

Parkinson disease (PD) etiology is closely linked to the aggregation of α -synuclein (α S). Copper(II) ions can bind to α S and may impact its aggregation propensity. As a consequence, deciphering the exact mode of copper(II) binding to α S is important in the PD context. Several previous reports have shown some discrepancies in the description of the main copper(II) site in α S, which are resolved here by a new scenario. Three Cu^{II} species can be encountered depending on the pH and the Cu to α S ratio. At low pH, Cu^{II} is bound to the N-terminal part of the protein by the N-terminal amine, the adjacent deprotonated amide group of the Asp2 residue, and the carboxylate group from the side chain of the same Asp2. At pH 7.4, the imidazole group of remote His50 occupies the fourth labile equatorial position of the previous site. At high Cu^{II} over α S ratio (>1), His50 leaves the coordination sphere of the first Cu site centered at the N-terminus, because a second weak affinity site centered on His50 is now filled with Cu^{II}. In this new scheme, the remote His plays the role of a molecular switch and it can be anticipated that the binding of the remote His to the Cu^{II} ion can induce different folding of the α S protein having various aggregation propensity.

Introduction

α -Synuclein (α S) is a 140 amino acid residue protein implicated in the pathogenesis of severe neurodegenerative disorders known as synucleinopathies, including Parkinson's disease (PD) and dementia with Lewy's bodies.¹⁻⁴ α S, together with β - and γ -synuclein

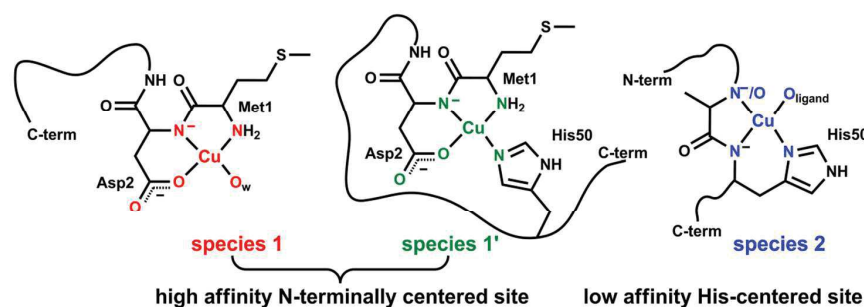
belongs to the synuclein protein family. While γ S does not seem to be involved in neurodegenerative disorders (but may be involved in various types of cancers⁵⁻⁸), β S is considered as the α S aggregation antagonist and it might play a preventing key role in the neurodegenerative cascade.⁹⁻¹⁵ β S and α S are both co-localized in the pre-synaptic nerve terminals and are considered as intrinsically disordered proteins in solution.¹⁶⁻²⁰ The main difference between the two proteins is the presence of the NAC (non-amyloid component) region in α S only. Interestingly, that region is considered responsible for α S aggregation, leading to the formation of parallel β -sheet rich fibril structures.^{2, 21-23}

Over the last decade, the role of metal ions in α S aggregation has been taken seriously into account by considering that (i) an alteration of metal homeostasis always occurs in patients affected by neurodegenerative disorders,²⁴⁻²⁶ and that (ii) α S is able to bind physiological metal ions like copper, iron and zinc.²⁷⁻²⁹ Imbalance of metal ion homeostasis is one of the pathological hallmarks of PD, together with the presence of protein-based fibrillar inclusions inside (Lewy's bodies) or outside neuronal cells of the *substantia nigra*. Although it is still not clear if metal dyshomeostasis is a starting or ending point of neurodegeneration, metal ions may contribute either to self-oligomerization of α S or, when redox active, to the production of highly reactive oxygen species (ROS).

It is nowadays well accepted that copper coordination to α S increases its aggregation ability and enhances its toxicity *in vivo* and *in vitro*,^{30, 31} in particular, it induces the formation of copper(II)-mediated oligomeric forms of α S which are the most toxic species able to dramatically induce cell death *in vivo*.³² Most of investigators agree with Cu^{II} anchoring to the N-terminal region of α S with higher affinity than in the C-term part.³³ Recent evidence showed that this N-terminal anchoring is logically lost when the protein undergoes N-terminal post-translational acetylation.³⁴ In that latter case, the Cu^{II} site has been localized in the His50 region and the physiological relevance of Cu^{II} binding to the N-acetylated synuclein discussed. Copper-coordinated β S or γ S shows no aggregation ability and relatively no toxicity *in vivo*.³² In contrast to copper, iron-mediated α S oligomers do not seem to be as toxic.³² Moreover, coordination to redox active metal ions like the $\text{Cu}^{\text{II}}/\text{Cu}^{\text{I}}$ couple can lead to the production of ROS, in the presence of molecular oxygen and ascorbic acid that can lead to extensive cellular damages and accelerate neurodegeneration evolution.^{28, 34-36} The link between oxidative stress (probably mediated by redox metal ions) and PD is supported by postmortem analysis that show oxidative stress-mediated neuronal cell degeneration.³⁷

In this context the exact copper coordination to both α S and β S assumes important significance and has first to be clarified. Copper(II) binding to α S and to a lesser extent β S

has been extensively studied in the last ten years.³³ However, while implication of the two N-terminal amino-acid residues, namely Met1 and Asp2, in the higher affinity site is consensual, there is still a main controversy on the exact nature of this Cu^{II} binding site. As recently reviewed in³³ and discussed in most of the reports on this issue,^{30, 38-48} two propositions have emerged. The copper coordination modes will be referred to here as a “species” that correspond to Cu^{II} ions bound to a specific “site”. Site/species 1 and site/species 1' correspond to a Cu^{II} ion bound to the N-terminal amine, the adjacent deprotonated amide function of Asp2, and the carboxylate side-chain of Asp2, the fourth equatorial position being occupied by a water molecule or by the remote His (His50 in α S or His65 in β S), respectively (Scheme 1). The presence and nature of apical ligands have not been investigated yet. A second weak affinity site (site 2) centered on the remote His has also been identified. In this species, near pH 7.5, the Cu^{II} ion is bound by the imidazole (Im) group of the His residue, one or two adjacent deprotonated amide functions from the N-terminal side and oxygen donor atoms (Scheme 1, right).⁴⁴ The two former species can be distinguished by their EPR parameters, as reminded in Table 1, with a g_{\parallel} of 2.24 and $A_{\parallel}({}^{63}\text{Cu})$ of $190 \pm 5 \text{ } 10^{-4} \text{ cm}^{-1}$ for Cu^{II} in site 1, g_{\parallel} of 2.22 and $A_{\parallel}({}^{63}\text{Cu})$ of $180 \pm 5 \text{ } 10^{-4} \text{ cm}^{-1}$ for Cu^{II} in site 1'. From an overview of Table 1, it appears that Cu^{II} binding to both high affinity sites, 1 and 1', can occur depending on the experimental conditions. Therefore, we wondered whether the apparent discrepancy of literature data could be unified in a new scenario that takes into account the importance of external stimuli such as pH or Cu: α S ratio. In this paper, we thus propose a new scenario that reconciles most, if not all, of published data on Cu^{II} binding to α S, a very important issue to better decipher the impact of copper(II) ions in PD.



Scheme 1. Species 1, 1' and 2 corresponding to Cu^{II} binding into the high-affinity N-terminal amine-centered site (left) and to the His50-centered site (right), respectively. Regarding species 2, in the present work, the 2N2O equatorial coordination mode is predominant at pH 7.3 while in the work of Kowalik,⁴⁴ the 3N1O mode was detected as the major species. Note that structure of species 2 is in line with Cu^{II} binding domain observed in Ac- α S.³⁴ Note that, in general, when the His residue is involved in the formation of a metallacycle, binding occurs via the N_δ (to favor the most stable metallacycle), else it mainly occurs via the N_ε (due to a less steric constraint).⁴⁹

Table 1. EPR parameters of the different Cu^{II} binding sites in αS and model peptides.

peptides	g//	A _{//} (10 ⁻⁴ cm ⁻¹)	conditions	Values for	ref.
Site 1 (2N2O)					
αS	2.24(5) ^[a]	191 ± 5 ^[a]	300 μM, 20 mM MES buffer, 100 mM NaCl, pH 6.5 and 5.0	^{63/65} Cu	30
αS	2.24(6)	185 ± 5	350 μM in PBS buffer, pH 7.4, in mixture with site 1'	⁶³ Cu ^[b]	41
H50N-αS			350 μM in PBS buffer, pH 5.0,		
			350 μM in PBS buffer, pH 7.4 and 5.0		
αS	2.25	189 ± 5	500-700 μM, 20mM MES, 20 mM MOPS buffer, 100 mM NaCl, pH 6.5	^{63/65} Cu	38
H50A-αS	2.25				39
αS(1-6)	2.25				
H50Q-αS(1-99)	2.24(0) ^[a]	193 ± 5 ^[a]	450 μM, 20 mM MES buffer pH 6.8	^{63/65} Cu	40
αS, H50A	2.24(2)	185 ± 5	25 mM MOPS buffer, pH 7.4	^{63/65} Cu	42
αS(1-10)	2.24(5)	192 ± 5			
αS(1-17/28/30/39)	2.24(6)	193 ± 5	0.8-1.5 mM, pH 4.5 to 8.5	^{63/65} Cu	45
MD-αS(31-56)	2.24(2)	193 ± 5	pH 5.5	^{63/65} Cu	44
αS(1-15) ^[b,c]	2.248	190 ± 5	400 μM, 50mM Hepes buffer pH 7.3	⁶³ Cu	this work
αS(1-15) +Ac-αS(45-55) ^[b,c]	2.248	190 ± 5	400 μM, no buffer pH 6.0	⁶³ Cu	this work
Site 1' (3N1O)					
αS(1-140)	2.22(8)	179 ± 5	350 μM in PBS buffer, pH 7.4, in mixture with site 1	⁶³ Cu	41
αS(1-99)	2.22(4) ^[a]	185 ± 5 ^[a]	25 mM MOPS buffer, pH 7.4	^{63/65} Cu	42
αS	2.22(6) ^[a]	186 ± 5 ^[a]			
αS(1-56)	2.22(9) ^[a]	180 ± 5 ^[a]			
αS(1-97)	2.22(6) ^[a]	186 ± 5 ^[a]			
MD-αS(31-56)	2.22(7)	185 ± 5	pH 7.4	^{63/65} Cu	44
αS(1-15)+Im	2.230	180 ± 5	400 μM, 50mM Hepes buffer pH 7.3	⁶³ Cu	this work
αS(1-15)+					
Ac-αS(45-55) ^[b,c]					
Site 2					
Ac-MD-αS(41-56)	2.22(6)	172 ± 5	pH 7.5, no buffer	^{63/65} Cu	44
Ac-αS(45-55) ^[b,c,d]	2.277	174 ± 5	400 μM, 50mM Hepes buffer pH 7.3	⁶³ Cu	this work
	2.228	171 ± 5			

^[a] Values from measurement on the EPR spectrum in Figures of the paper.

^[b] Values from simulations (See Figure S1 and table S1 in the Supporting Information for further details).

^[c] The experiments were performed using ⁶⁵Cu but the values given in Table 1 and in the text were recalculated for the most abundant ⁶³Cu isotope, to allow a more direct comparison with data obtained with mixture of ⁶³Cu/⁶⁵Cu in their natural abundance.

^[d] In the work of Kowalik, the major species at pH 7.5 is the 3N1O species containing two deprotonated amide functions, while in the present work this species is detected in weaker proportion. In contrast, the 2N2O species (containing only one deprotonated amide group) is predominant under our experimental conditions.

Results

1-EPR and CD spectroscopy of copper(II)- α S model peptide complexes

Investigations were performed on simple models for each of the sites defined above, that is: (i) peptide α S(1-15) (sequence: MDVFMKGLSKAKEGV) encompassing the 15 N-terminal amino-acid residues of α S for site 1, peptide α S(1-15) plus imidazole or an imidazole containing molecule for site 1' and peptide Ac- α S(45-55) (sequence: KEGVVHGVATV-NH₂, A53T) containing His50 for site 2^a. First, we have validated by EPR that these systems were correct models of the three sites. In Figure 1-top, the three EPR signatures of Cu^{II} bound to those peptides at pH 7.3 are thus plotted and the EPR parameters are reported in Table 1^b. The EPR signatures of Cu^{II} in site 1 and 1' are not so different ($g_{\parallel} = 2.248$, $A_{\parallel} = 190 \pm 5 \text{ } 10^{-4} \text{ cm}^{-1}$ and $g_{\perp} = 2.230$, $A_{\perp} = 180 \pm 5 \text{ } 10^{-4} \text{ cm}^{-1}$, respectively, see Figure S1 and table S1 in the Supporting Information for further details) and they perfectly reproduce those of the corresponding species reported in the literature. Species 1' is characterized by a small up-field shift of the hyperfine lines and a decrease in the hyperfine coupling compared to species 1, thus leading to a position of the fourth "overshoot" hyperfine line that is identical for both species. Superhyperfine coupling can be observed on the perpendicular transition for species 1 but not for 1'. It is worth noting that we have used isotopically pure ⁶⁵Cu to maximize the observed differences in the EPR spectra and that they are still weak and can thus be hardly detectable with use of mixture of ⁶³Cu/⁶⁵Cu in their natural abundance. Circular dichroism (CD) was also often used to characterize Cu^{II} binding to synuclein. For this reason, the three CD fingerprints of Cu^{II} bound in the three model sites have been plotted in Figure 1-bottom. On one hand, spectrum of Cu^{II}-Ac- α S(45-55) is clearly different from those of species 1 and 1', both in the d-d and in the charge transfer regions. It is also different from the CD spectra of the Ac- α S protein recently published.³⁴ This is because CD data on the protein where acquired at pH 6.5, a pH where the Cu^{II} affinity for the His50 centered site is so weak (about $8 \text{ } 10^3 \text{ M}^{-1}$, see Table 3) that the complex is significantly dissociated. On the other hand, there is only a very subtle difference between the spectra of species 1 and 1', with a small blue shift of the d-d envelope and the appearance of a weak positive CD feature near 350 nm for the complex in the presence of imidazole (species 1'), in line with the replacement of the oxygen atom of the water molecule by the nitrogen atom of the imidazole ring.⁵⁰ CD spectra

^a The mutation A53T was shown not to affect Cu(II) coordination in site 2, see ref. 48.

^b The experiments were performed using ⁶⁵Cu but the values given in Table 1 and in the text have been recalculated for the most abundant ⁶³Cu isotope, to allow a more direct comparison with data obtained with mixture of ⁶³Cu/⁶⁵Cu in their natural abundance.

of both species 1 and 1' are both close to the one of the α S protein,³⁴ and because of their high similarity, it is not possible to tell which one resembles more the CD spectrum of the protein. It thus appears that EPR is a more suitable and reliable technique to investigate Cu^{II} binding to site 1 or site 1' than CD. In the following we will thus focus on EPR. Generally speaking, this is a very powerful technique to decipher Cu(II) binding to flexible peptides.^{51, 52}

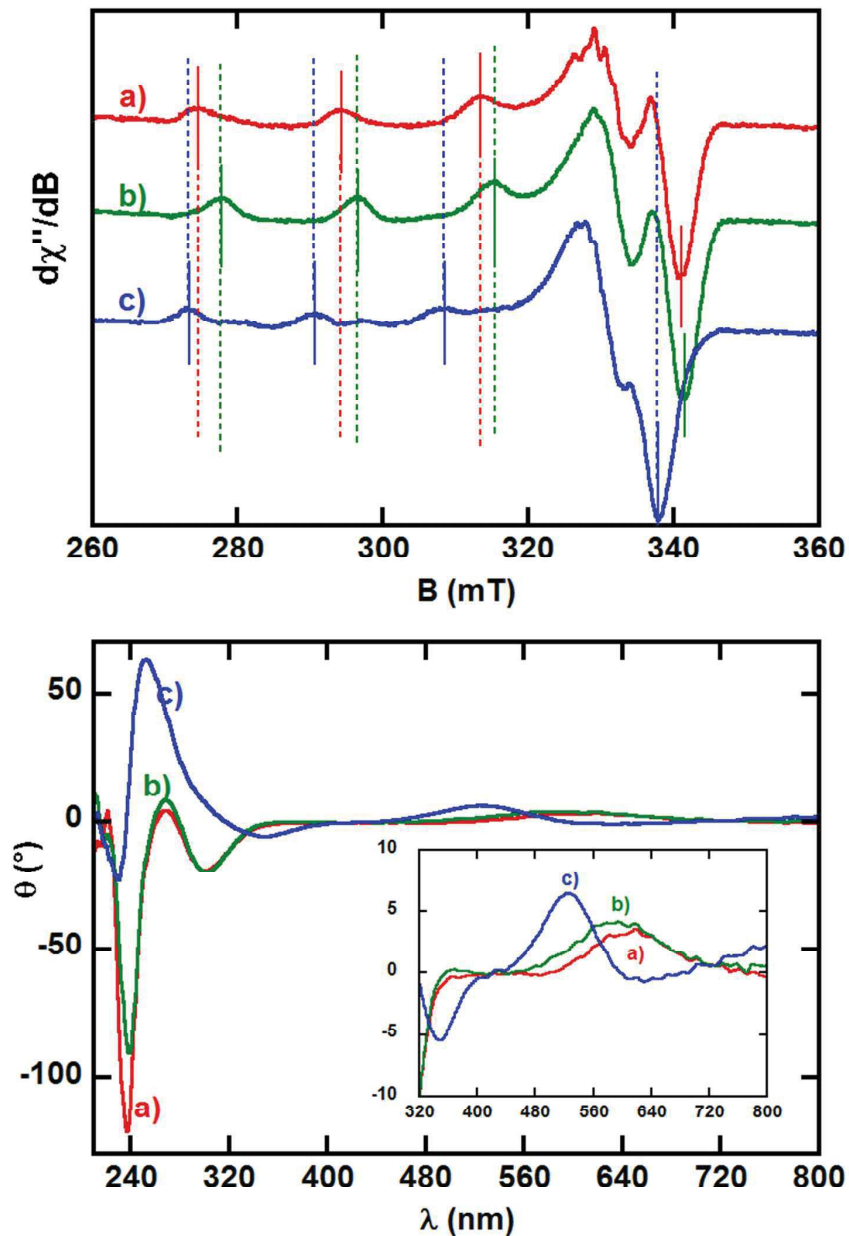


Figure 1. EPR (top) and CD (bottom) spectra of Cu^{II} bound to peptide α S(1-15) (a, red), peptide α S(1-15) + 1 equiv. of Im (b, green) and to peptide Ac- α S(45-55) (c, blue). Top, experimental conditions: [α S(1-15)], [Im] or [Ac- α S(45-55)] = 400 μ M, [⁶⁵Cu(II)] = 360 μ M (0.9 equiv.) in 50 mM Hepes buffer pH 7.3, 10% (v/v) of glycerol at 120 K; bottom, experimental conditions: [α S(1-15)], [Im] or [Ac- α S(45-55)] = 400 μ M, [Cu(II)] = 360 μ M (0.9 equiv.) in 50 mM Hepes buffer pH 7.3 at 25°C, ℓ =1 cm.

2-pH dependence of the EPR copper(II) signal in the presence of α S model peptides.

The EPR signatures of Cu^{II} bound to a 1:1 mixture of $\alpha\text{S}(1-15)$ and $\text{Ac-}\alpha\text{S}(45-55)$ (0.9:1:1 $\text{Cu}:\alpha\text{S}(1-15):\text{Ac-}\alpha\text{S}(45-55)$ ratio) as a function of pH are plotted in Figure 2. The evolution from pH 5.5 to pH 7.3 shows that the $\text{Cu}(\text{II})$ species changes progressively from species 1 to 1', with the two species being in equal quantity near pH 6.0 (Figure 2c). This is in line with the deprotonation of the remote His (pK_a close to 6.5⁴⁴) and its subsequent binding to Cu^{II} .

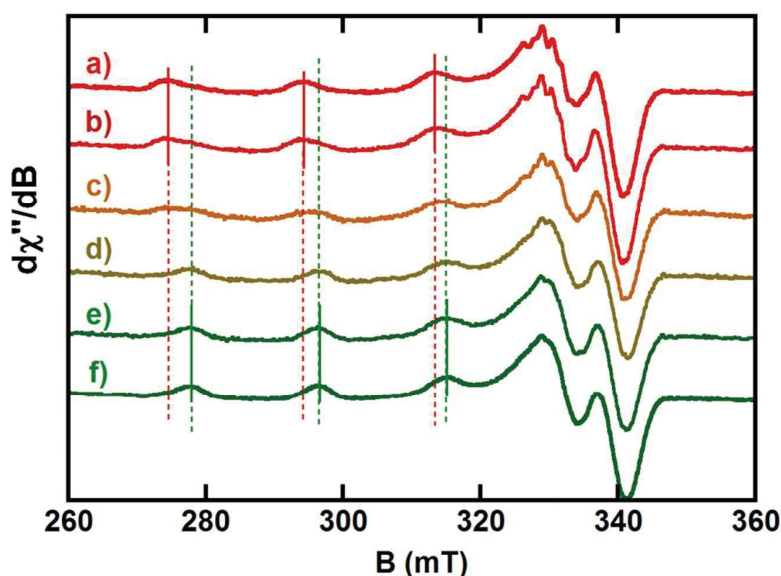


Figure 2. EPR spectra of Cu^{II} bound to peptides $\alpha\text{S}(1-15)$ and $\text{Ac-}\alpha\text{S}(45-55)$ as a function of pH: 5.5 (b), 6.0 (c), 6.5 (d), 7.0 (e) and 7.3 (f). Spectrum (a) corresponds to Cu^{II} bound to $\alpha\text{S}(1-15)$ at pH 7.3. Recording conditions: $[\alpha\text{S}(1-15)]$ or $[\text{Ac-}\alpha\text{S}(45-55)] = 400 \mu\text{M}$, $[\text{Cu}^{\text{II}}] = 360 \mu\text{M}$ (0.9 equiv.), 10% (v/v) of glycerol at 120 K. For samples from b) to e) pH was adjusted with the use of a NaOH stock solution (1 mM) to obtain desired values; the pH was controlled before and after the EPR measurements. For samples a) and f) 50 mM Hepes buffer was used to maintain a pH of 7.3.

3-Effect of Cu^{II} molar ratios

Then, we performed a second experiment at pH 7.3 in which the Cu ratio was increased from 0.9 to 2 with regards to a 1:1 mixture of $\alpha\text{S}(1-15)$ and $\text{Ac-}\alpha\text{S}(45-55)$. The corresponding EPR spectra are plotted in Figure 3, top. With the increase of $\text{Cu}:\alpha\text{S-peptides}$ ratio, the EPR spectrum evolves from a species with 1'-like signature (compare spectra a and b) to a combination of species with 1 and 2 signatures (compare spectrum d with spectra e and f), as shown by the down-field shift of the hyperfine lines. This evolution can be even more clearly demonstrated by the calculation of spectrum d, using a linear combination of spectra e (50%) and f (50%) corresponding to Cu^{II} bound in sites 1 and 2, respectively (Figure 4, a).

1
2
3
4
5
6
7
8
9
10
11
12
13
14
15
16
17
18
19
20
21
22
23
24
25
26
27
28
29
30
31
32
33
34
35
36
37
38
39
40
41
42
43
44
45
46
47
48
49
50
51
52
53
54
55
56
57
58
59
60

Such an evolution agrees with the affinity of the N-centered sites (1 or 1') being higher than those of the His-centered site (site 2), since site 2 is filled in a second time (see Table 3). Reproduction of spectrum b in Figure 4 by a linear combination of Cu^{II} in site 1, site 1' and site 2 will be commented on in the discussion part.

We have also monitored the same experiment by CD (Figure 3, bottom). The results are in line with those obtained by EPR. However, the CD signatures of species 1 (spectrum a) and 1' (spectrum b) are so close that linear combinations of either a) or b) with that of species 2 (spectrum c) both reproduce satisfactorily the spectrum of a mixture of αS(1-15), Ac-αS(45-55) and Cu^{II} in a 1:1:2 ratio (spectrum d). Hence CD, in contrast to EPR, does not allow one to discriminate the nature of the high affinity binding site when both high and weak affinity sites are occupied.

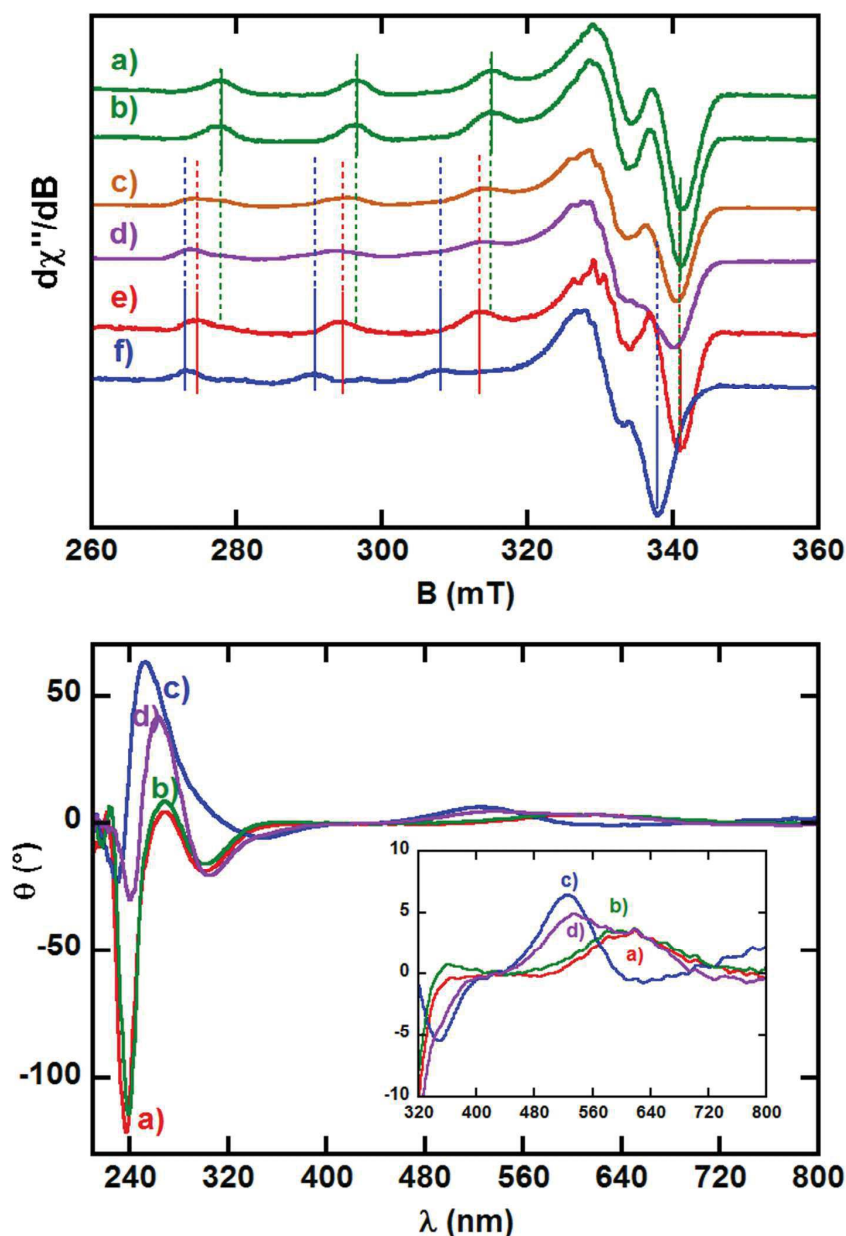


Figure 3. Top: EPR spectra of Cu^{II} bound to mixtures of peptides $\alpha\text{S}(1-15)$ and $\text{Ac-}\alpha\text{S}(45-55)$ as a function of the αS -peptides: Cu^{II} ratio at pH 7.3 (b) 1.0 [$\alpha\text{S}(1-15)$] : 1.0 [$\text{Ac-}\alpha\text{S}(45-55)$] : 0.9 [$\text{Cu}(\text{II})$] ; (c) 1.0 [$\alpha\text{S}(1-15)$] : 1.0 [$\text{Ac-}\alpha\text{S}(45-55)$] : 1.5 [$\text{Cu}(\text{II})$] and (d) 1.0 [$\alpha\text{S}(1-15)$] : 1.0 [$\text{Ac-}\alpha\text{S}(45-55)$] : 2.0 [$\text{Cu}(\text{II})$]. Spectrum (a) corresponds to $\text{Cu}(\text{II})$ bound to peptide $\alpha\text{S}(1-15)$ + 1 equiv. of Im, spectra (e) to Cu^{II} bound to peptide $\alpha\text{S}(1-15)$ and (f) Cu^{II} bound to peptide $\text{Ac-}\alpha\text{S}(45-55)$ at pH 7.3. Bottom: CD spectra of Cu^{II} bound to peptide $\alpha\text{S}(1-15)$ and $\text{Ac-}\alpha\text{S}(45-55)$ as a function of the $\text{Cu}(\text{II})$ ratio with respect to the peptides at pH 7.3. (b) 1.0 [$\alpha\text{S}(1-15)$] : 1.0 [$\text{Ac-}\alpha\text{S}(45-55)$] : 0.9 [$\text{Cu}(\text{II})$] and (d) 1.0 [$\alpha\text{S}(1-15)$] : 1.0 [$\text{Ac-}\alpha\text{S}(45-55)$] : 2.0 [$\text{Cu}(\text{II})$]. Spectra (a) correspond to Cu^{II} bound to peptide $\alpha\text{S}(1-15)$ and (c) to Cu^{II} bound to peptide $\text{Ac-}\alpha\text{S}(45-55)$ at pH 7.3. Top, recording conditions: [$\alpha\text{S}(1-15)$] or [$\text{Ac-}\alpha\text{S}(45-55)$] = 400 μM , [$^{65}\text{Cu}(\text{II})$] = 360 μM (0.9 equiv.), 600 μM (1.5 equiv.) and 800 μM (2.0 equiv.) in 50 mM HEPES buffer, 10% (v/v) of glycerol at 120 K for spectra b, c and d respectively; bottom, [$\alpha\text{S}(1-15)$] or [$\text{Ac-}\alpha\text{S}(45-55)$] = 400 μM , [$^{65}\text{Cu}(\text{II})$] = 360 μM (0.9 equiv.), and 800 μM (2.0 equiv.) in 50 mM HEPES buffer at 25°C, $\ell=1$ cm.

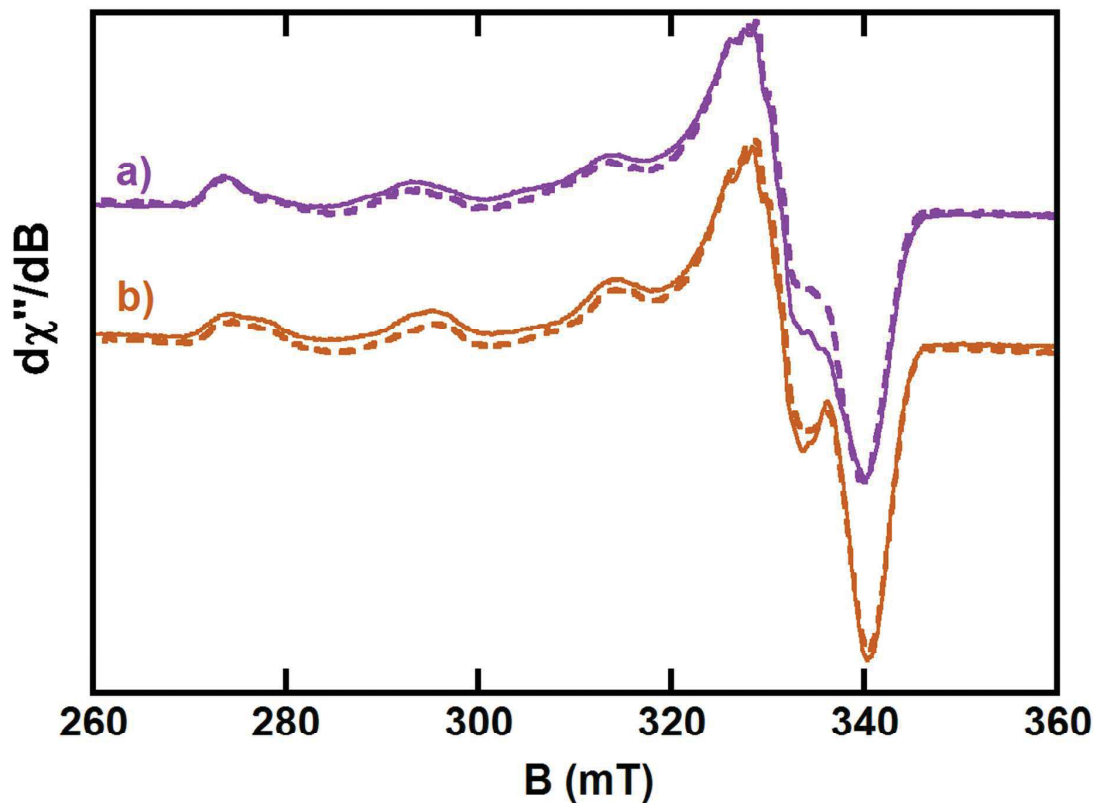


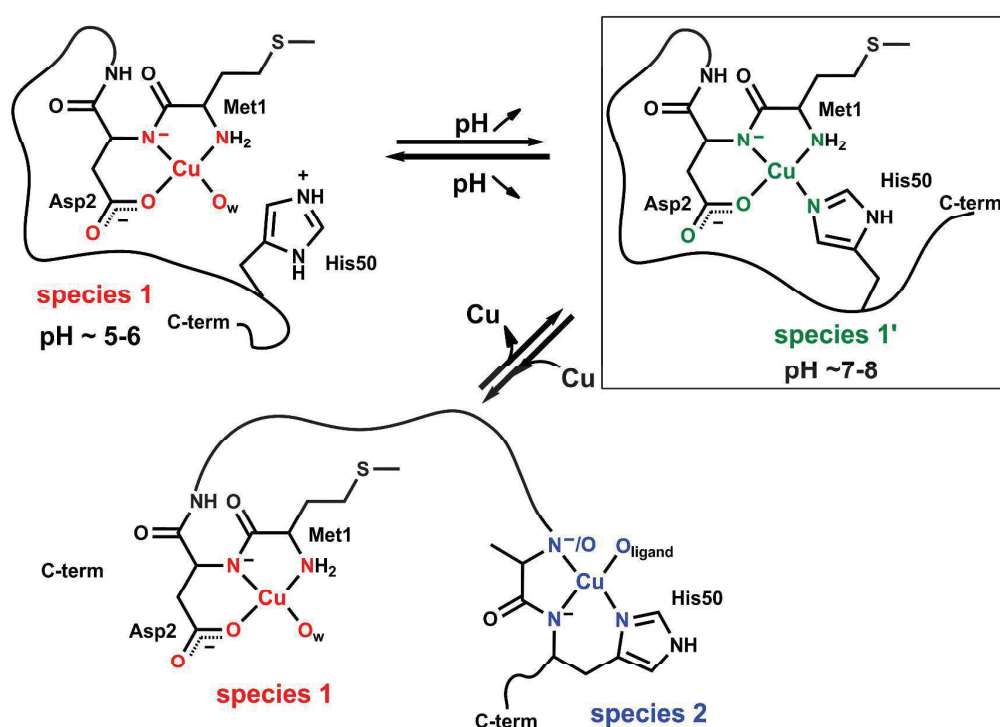
Figure 4. Reproduction of spectra (d) and (c) from Figure 3, using a linear combination of EPR spectrum of Cu^{II} in site 1 and site 2 (a) and a linear combination of Cu^{II} in site 1, site 1' and site 2 (b). Linear combination is shown as dotted lined.

Discussion

1-A new scenario for copper(II)- α S coordination

The scenario depicted in Scheme 2, which has not been proposed in the literature yet, explains the results detailed above. At pH 7.3, Cu^{II} binds to site 1', made of the N-terminal portion of α S and the remote His50. When the pH is decreased, His becomes protonated and is released from the Cu^{II} center leading to species 1. When the Cu: α S peptide ratio is increased at neutral pH, the weak Cu^{II} site centered on His50 (site 2) is filled up, thus inducing concomitant release of His50 from species 1' leading to formation of species 1. Thus species 1 can be formed either at lower pH or at Cu- α S ratio >1. The former possibility might be more biologically relevant as (i) the Cu^{II} affinity for site 2 is low and (ii) pH around 5-6 can occur in certain biological compartments, such as intracellular location, including endosomes and lysosomes, in which the α S protein is present.^{53, 54}

This scenario is confirmed by the fact that a combination of EPR signatures of species 1, 1' and 2 with the same relative weight reproduces perfectly the EPR spectrum obtained by mixing α S(1-15), Ac- α S(45-55) and Cu^{II} in a 1:1:1.5 ratio (Figure 4, b). Indeed, in superstoichiometric ratio of Cu^{II} , the low affinity site 2 has to be filled with 0.5 equiv. of Cu^{II} and this requires 0.5 of His50. Thus only 0.5 equiv. of His50 is available to bind Cu^{II} in the high affinity site, leading to 0.5 equiv. of species 1'. The remaining 0.5 equiv. of Cu^{II} is thus finally bound to site 1. Details of Cu^{II} occupation of sites 1, 1' and 2 as a function of Cu equivalents are given in Table 2.



Scheme 2. Proposed role of His50 in modulating Cu^{II} binding sites in α S. Note that the same situation may apply for His65 and β S.

Table 2. Repartition of Cu in the three sites as a function of the Cu equivalents at pH 7.3.

Cu^{II} equiv.	Site 1	Site 1'	Site 2	His50-bound in site 1'	His50-bound in site 2
0.5	0	0.5	0	0.5	0
1	0	1	0	1	0
2	1	0	1	0	1
1.5	0.5	0.5	0.5	0.5	0.5

2-A review of the published results in the light of the new scenario proposed.

At pH 7.3 the first anchor of Cu^{II} binding to α S is the N-terminal amine leading to site 1' where the equatorial Cu^{II} coordination is completed by the deprotonated amide function of Asp2, the side-chain of Asp2 and the remote His50 at pH 7.3. This model agrees with the majority of published data, which support His-binding to Cu^{II} in α S. Indeed, most articles report His binding to Cu^{II} at a Cu: α S ratio of 1:1 and pH 7.3.^{30, 41, 42, 44} The main argument comes from EPR spectra obtained using α S mutants at His50, where a shift similar to the one observed here was obtained in the EPR signatures (due to switching to site 1) or by pulsed EPR techniques with site specific labeling.⁴⁰⁻⁴² This scenario is also in line with the NMR data that show a line broadening of His50 at substoichiometric Cu^{II} to α S ratio,^{30, 38, 47} and with the potentiometric studies with the model peptides α S(1-17/28/30/39) and MD- α S(31-56).^{44, 45}

Actually, the data reported by Drew⁴¹, where both species 1 and 1' are detected by EPR near pH 7 can be easily explained by considering a pH decrease due to the use of PBS buffer, the pH of which decreases significantly upon freezing.⁵⁵ This will result in the mixture of species 1 and 1' as observed.⁴¹ Regarding the EPR data by Binolfi,^{33, 39} they were obtained at pH 6.5, where the two species coexist, and using ^{63/65}Cu. Under these conditions, difference in the EPR signatures can be overseen. It is thus important to use isotopically pure ⁶⁵Cu like in the present study or in the study by Drew to obtain narrower and better spaced hyperfine lines, enhancing the differences between the EPR signatures of the two species 1 and 1'.

This new scenario also explains the CD data showing that a second Cu equivalent can be bound to wt- α S but not to the His50 mutant.³⁸ The conclusion that His50 is not involved in the high affinity site at pH 7.3 was based on the apparent unchanged CD signature of the high affinity site during the loading of the weak affinity site. However, as shown here, due to the high similarity between species 1 and 1' CD fingerprints, modification of the signature of the N-terminally centered high affinity site in presence of site 2 cannot be properly monitored by CD, but can be by EPR (as shown in Figure 3) and EPR shows that His is bound.

Additionally, the model proposed here is in line with the affinity measurements performed on α S and α S mutants at His50, or smaller peptidic models of them, showing that systems containing His50 bear higher affinity for Cu^{II}, thus indicating participation of His (i.e. site 1' is the main site at pH 7.3). More precisely, literature data are contradictory with conditional affinity constant values (i.e. absolute values at a given pH, pH 7.3 here) spanning from 10⁶ M⁻¹ to 10¹⁰ M⁻¹.³³ We have excluded values below 10⁹ M⁻¹, which are apparent

values not corrected for the buffer contribution (competition of buffer for Cu^{II} binding can significantly decrease the determined affinity values). Remaining values are reported in Table 3. Competition experiments with the pentaglycine as external chelator or oxidized glutathione chelator give dissociation constant values in nM range, with a four times higher affinity for wild-type αS compared to the H50A mutant.⁴² Another accurate data come from the potentiometry studies of peptide $\alpha\text{S}(1-17)$ corresponding to site 1 and to peptide MD- $\alpha\text{S}(31-56)$ (i.e. the sequence of αS centered on His50 + the two key N-terminal amino-acid residues) corresponding to site 1'.^{44, 45} At pH 7.4, affinity of Cu^{II} for the former peptide is about five times weaker than for the latter peptide. It is also interesting to note that when the pH is decreased the difference of Cu^{II} affinity between the two peptides tends to disappear in line with the release of the His ligand at lower pH, leading to formation of a site 1 (instead of 1') in the latter peptide (Table 3). This difference, while significant, has not been detected neither by Trp fluorescence of $\alpha\text{S}(\text{F4W})$ and $\alpha\text{S}(\text{F4W}, \text{H50A})$ nor by ITC.^{39, 43, 46, 56} This may be due to the fact that these techniques are less suitable for the determination of such a high affinity constant, which thus requires performing the experiments at very low concentrations (here, < 100 nM). It is also worth noting that affinity of Cu^{II} for the Ac- $\alpha\text{S}(45-55)$ peptide, used to model site 2 is significantly weaker than for species 1 or 1', in line with above described spectroscopic data. This effect is particularly obvious at low pH (pH 6.5) where there are more than 4 orders of magnitude between the affinity values.

Table 3. Dissociation and corresponding affinity constants calculated from literature data.

peptide	site	pH	K_d (nM)	K_a 10^9	refs.
wt- αS	1'	7.4	0.11 ^[a] /0.15 ^[b]	9.1/6.7	42
$\alpha\text{S}(\text{His50A})$	1		0.40 ^[a] /0.60 ^[b]	2.5/1.7	
MD- $\alpha\text{S}(31-56)$	1'		0.19	5.32	44
$\alpha\text{S}(1-17)$	1		0.94	1.06	45
Ac- $\alpha\text{S}(45-55)$	2		2.54 10^3	0.39 10^{-3}	48
MD- $\alpha\text{S}(31-56)$	1'	7.0	1.19	0.84	44
$\alpha\text{S}(1-17)$	1		4.01	0.25	45
MD- $\alpha\text{S}(31-56)$	1'	6.5	14.7	0.068	44
$\alpha\text{S}(1-17)$	1		30.7	0.033	45
Ac- $\alpha\text{S}(45-55)$	2		0.12 10^6	8.3 10^{-6}	48
MD- $\alpha\text{S}(31-56)$	1'	6.0	195	5.13 10^{-3}	44
$\alpha\text{S}(1-17)$	1		275	3.64 10^{-3}	45

^[a] From competition with pentaglycine

^[b] From competition with glutathione

3-Possible formation of ternary copper(II)-(α S)₂ complexes.

In the course of our experiments, we have also investigated the possibility of forming ternary species with site 1 plus imidazole containing molecules (Figure 1, Figure S2-S3). It clearly appears that species 1 can form easily ternary complexes with imidazole containing molecules occupying the fourth labile equatorial position but not more position (Figure S4). Thus, species 1 could make ternary complexes with amino acids or other His containing proteins and perhaps most importantly with His50 from another α S (or β S) molecules. This would lead to a Cu-bridged synuclein dimer, which could have an important impact on the aggregation behavior.³⁰

Concluding remarks.

The Cu^{II} binding scenario to α S reported in the present paper reconciles most of the previously published studies on the same subject. It is strongly supported by EPR monitoring of Cu^{II} binding to relevant model peptides of α S as a function of pH and Cu to peptides ratio. In this new model of Cu^{II} binding to α S, the role of His50 appears to be crucial. We thus anticipated that it can act as a molecular switch and induces different folding of the α S protein, when involved in site 1' (substoichiometric ratio of Cu^{II} to α S, pH > 6.5), site 2 (superstoichiometric ratio of Cu^{II} to α S, pH > 6.5) or not involved at all (pH < 6.5). This may thus impact the aggregation properties of the α S protein. Additionally, ternary species α S-Cu^{II}- α S' or α S-Cu^{II}-(Ac- α S), with the Cu^{II} ion bridging two different protein molecules (α S being bound by its N-terminal part and α S' or Ac- α S being bound by the His50) is also possible and this may impact aggregating properties as well, where the proteins aggregation has been widely acknowledged as a key event in the aetiology of PD. In case of Ac- α S, the impact of Cu^{II} on aggregation of Ac- α S, has been recently shown to be only minor.³⁴ However, formation of mixed peptides complex α S-Cu^{II}-(Ac- α S) is conceivable and its consequences on aggregation might contribute to the biological relevance of the interaction of Ac- α S with Cu^{II}.

Materials and Methods

Peptide and reagents.

α S(1-15), Ac- α S(45-55, A53T) and β S(1-15) peptides were synthesized on solid phase using Fmoc chemistry. Rink-amide resin was used as the solid support, so that the resulting peptides would be amidated at the C-terminus. After removal of the peptide from the resin and deprotection, the crude product was purified by RP HPLC on a Phenomenex Jupiter Proteo C12 column, using a Jasco PU-1580 instrument with diode array detection (Jasco MD-1510), with a semi-linear gradient of 0.1% trifluoroacetic acid (TFA) in water to 0.1% TFA in CH₃CN over 40 min. The identity of the peptide was confirmed by Electrospray ionization mass spectrometry (Thermo-Finnigan). The purified peptide was lyophilized and stored at -20°C until use.

α S(1-15), β S(1-15) and Ac- α S(45-55) lyophilized peptides were weighed and dissolved in pure water to obtain three high concentration stock solutions. The stock solution concentration of both α S(1-15) and β S(1-15) was titrated by UV-Vis absorption monitoring the phenylalanine absorption peak at 258 nm (typical of Phe-containing peptides) with a molar extinction coefficient of 195 M⁻¹cm⁻¹, obtaining a 1.80 mM and 2.57 mM stock solution for α S(1-15) and β S(1-15), respectively. For the Ac- α S(45-55) peptide, the concentration of the stock solution was measured through a Cu(II) titration in UV-Vis absorption by monitoring the growth of the d-d band at 580 nm at pH 8.0 (with the use of 50 mM Hepes buffer) due to the formation of the Cu(II)-amino/amido complex described by Valensin et al.⁴⁸ The obtained stock solutions were frozen and stored at -20 °C.

All other reagents were purchased from Sigma Aldrich.

CD spectroscopy.

CD Spectra were recorded at 25 °C with a JASCO J-815 spectropolarimeter equipped with a Perkin-Elmer temperature controller at a scan speed of 20 nm/min and 3 accumulations using a quartz cell with a 1 cm path length.

The acquired spectral window was between 200 and 900 nm with a band width of 1 nm, with a D.I.T. (data integration time) of 4 nm, a data pitch of 1 nm and standard sensitivity. Background spectrum was recorded with 50 mM Hepes buffer pH 7.3 in the same instrumental conditions and subtracted after the sample measurements.

pH was controlled after sample measurements (7.25 ± 0.05).

The obtained spectra were then smoothed with the Savitzky-Golay method.

Electron Paramagnetic Resonance (EPR).

EPR data were recorded using an Eleksys E 500 Bruker spectrometer, operating at a microwave frequency of approximately 9.5 GHz. All spectra were recorded using a microwave power of 20 mW across a sweep width of 150 mT (centered at 310 mT) with a modulation amplitude of 0.5 mT. Experiments were carried out at 120 K using a liquid nitrogen cryostat.

1
2
3
4
5
6
7
8
9
10
11
12
13
14
15
16
17
18
19
20
21
22
23
24
25
26
27
28
29
30
31
32
33
34
35
36
37
38
39
40
41
42
43
44
45
46
47
48
49
50
51
52
53
54
55
56
57
58
59
60

pH was controlled after sample measurements (7.25 ± 0.05). For pH-dependent measurements no buffer was used, pH was controlled after EPR measurements. pH is adjusted with NaOH or H₂SO₄ stock solution. Adjustment of pH in the EPR sample is performed with a micro-electrode pH-meter.

EPR simulations were performed by using the Easyspin software package⁵⁷ and routines written in the lab.

Acknowledgments.

We thank PRIN (Programmi di Ricerca di Rilevante Interesse Nazionale) (2010M2JARJ_004), CIRMMP (Consorzio Interuniversitario Risonanze Magnetiche di Metalloproteine Paramagnetiche), CIRCMSB (Consorzio Interuniversitario di Ricerca in Chimica dei Metalli nei Sistemi Biologici) for financial support and the French Infrastructure for Integrated Structural Biology (FRISBI) ANR-10-INSB-05-01. RDR and DV thank Prof. Stefano Mangani for supporting this project.

Supporting Information.

“EPR spectra and simulations of species I, I', II 2N2O component and 3N1O component) and corresponding EPR parameters; EPR and CD spectra of Cu(II) bound to α S(1-15) and β S(1-15) without and with one imidazole equivalent; EPR and CD spectra of Cu(II) bound to α S(1-15) and β S(1-15) with zero to three imidazole equivalents and EPR of Cu(II) bound to α S(1-15) plus one equiv. of imidazole containing ligands are available free of charge via the internet at <http://pubs.acs.org>.”

References.

1. Burke, R. E., *Neurologist* **2004**, *10*, 75.
2. Lucking, C. B.; Brice, A., *Cell. Mol. Life Sci.* **2000**, *57*, 1895.
3. El-Agnaf, O. M. A.; Irvine, G. B., *Biochem. Soc. T.* **2007**, *30*, 559.
4. Fink, A. L., *Acc. Chem. Res.* **2006**, *39*, 628.
5. Jia, T.; Liu, Y. E.; Liu, J.; Shi, Y. E., *Cancer Res.* **1999**, *59*, 742.
6. Ye, Q.; Huang, F.; Wang, X. Y.; Xu, Y. M.; Gong, F. S.; Huang, L. J.; Yang, C. K.; Zheng, Q. H.; Ying, M. G., *Oncol. Rep.* **2013**, *30*, 2161.
7. Wu, K. J.; Quan, Z. W.; Weng, Z. Y.; Li, F. M.; Zhang, Y. C.; Yao, X. H.; Chen, Y. D.; Budman, D.; D Goldberg, I.; Shi, Y. E., *Breast Cancer Res. Treat.* **2007**, *101*, 259.
8. Ahmad, M.; Attoub, S.; Singh, M. N.; Martin, F. L.; El-Agnaf, O. M. A., *FASEB J.* **2007**, *21*, 3419.
9. Masliah, E.; Rockenstein, E.; Veinbergs, I.; Sagara, Y.; Mallory, M.; Hashimoto, M.; Mucke, L., *Proc. Natl. Acad. Sci. U. S. A.* **2010**, *98*, 12245.
10. Rochet, J. C.; Conway, K. A.; Lansbury, P. T. J., *Biochemistry* **2000**, *39*, 10619.
11. Windisch, M.; Hutter-Paier, B.; Rockenstein, E.; Hashimoto, M.; Mallory, M.; Masliah, E., *J. Mol. Neurosci.* **2002**, *19*, 63.
12. Hashimoto, M.; Rockenstein, E.; Mante, M.; Mallory, M.; Masliah, E., *Neuron* **2001**, *32*, 213.
13. Masliah, E.; Hashimoto, M., *Neurotoxicology* **2002**, *23*, 461.
14. Israeli, E.; Sharon, R., *J. Neurochem.* **2009**, *108*, 465.
15. Rockenstein, E.; Hansen, L. A.; Mallory, M.; Trojanowski, J. Q.; Galasko, D.; Masliah, E., *Brain Res.* **2001**, *914*, 48.
16. Buchman, V. L.; Hunter, H. J.; Pinon, L. G.; Thompson, J.; Privalova, E. M.; Ninkina, N. N.; Davies, A. M., *J. Neurosci.* **1998**, *18*, 9335.
17. Yang, M. L.; Hasadsri, L.; Woods, W. S.; M., G. J., *Mol. Neurodegener.* **2010**, *5*, 1.
18. Uversky, V. N.; Oldfield, C. J.; Dunker, A. K., *Annu. Rev. Bioph.* **2008**, *37*, 215.
19. Marsh, J. A.; Singh, V. K.; Jia, Z.; D., F.-K. J., *Protein Sci.* **2006**, *15*, 2795.
20. Bertoncini, C. W.; Rasia, R. M.; Lamberto, G. R.; Binolfi, A.; Zbeckstetter, M.; Griesinger, C.; Fernandez, C. O., *J. Mol. Biol.* **2007**, *372*, 708.

21. Arima, K.; Ueda, K.; Sunohara, N.; Hirai, S.; Izumiyama, Y.; Tonozuka-Uehara, H.; Kawai, M., *Brain Res.* **1998**, *808*, 93.
22. Culvenor, J. G.; McLean, C. A.; Cutt, S.; Campbell, B. C. V.; Maher, F.; Jakala, P.; Hartmann, T.; Beyreuther, K.; Masters, C. L.; Li, Q. X., *Am. J. Pathol.* **1999**, *155*, 1173.
23. Chen, M.; Margittai, M.; Chen, J.; Langen, R., *J. Biol. Chem.* **2007**, *282*, 24970.
24. Allsop, D.; Mayes, J.; Moore, S.; Masad, A.; Tabner, B. J., *Biochem. Soc. T.* **2008**, *36*, 1293.
25. Lovell, M. A., *J. Alzheimers Dis.* **2009**, *16*, 471.
26. Bolognin, S.; Messori, L.; Zatta, P., *Neuromol. Med.* **2009**, *11*, 223.
27. Uversky, V. N.; Li, J.; Fink, A. L., *J. Biol. Chem.* **2001**, *276*, 44284.
28. Jomova, K.; Vondrakova, D.; Lawson, M.; Valko, M., *Mol. Cell. Biochem.* **2010**, *345*, 91.
29. Barnham, K. J.; Bush, A. I., *Curr. Opin. Chem. Biol.* **2008**, *12*, 222.
30. Rasia, R. M.; Bertoncini, C. W.; Marsh, D.; Hoyer, W.; Cherny, D.; Zweckstetter, M.; Griesinger, C.; Jovin, T. M.; Fernández, C. O., *Proc. Natl. Acad. Sci. U. S. A.* **2005**, *102*, 4294.
31. Paik, S. R.; Shin, H. J.; Lee, J. H.; Chang, C. S.; Kim, J., *Biochem. J.* **1999**, *340*, 821.
32. Wright, J. A.; Wang, X.; Brown, D. R., *FASEB J.* **2009**, *23*, 2384.
33. Binolfi, A.; Quintanar, L.; Bertoncini, C. W.; Griesinger, C.; Fernández, C. O., *Coord. Chem. Rev.* **2012**, *256*, 2188.
34. Moriarty, G. M.; Minetti, C. A.; Remeta, D. P.; Baum, J., *Biochemistry* **2014**, *53*, 2815.
35. Santner, A.; Uversky, V. N., *Metallomics* **2010**, *2*, 378.
36. Kowalik-Jankowska, T.; Rajewska, A.; Jankowska, E.; Wisniewska, K.; Grzonka, Z., *J. Inorg. Biochem.* **2006**, *100*, 1623.
37. Jenner, P., *Prog. Neurobiol.* **2003**, *53*, s26.
38. Binolfi, A.; Lamberto, G. R.; Duran, R.; Quintanar, L.; Bertoncini, C. W.; Souza, J. M.; Cerveñansky, C.; Zweckstetter, M.; Griesinger, C.; Fernández, C. O., *J. Am. Chem. Soc.* **2008**, *130*, 11801.
39. Binolfi, A.; Rodriguez, E. E.; Valensin, D.; D'Amelio, N.; Ippoliti, E.; Obal, G.; Duran, R.; Magistrato, A.; Pritsch, O.; Zweckstetter, M.; Valensin, G.; Carloni, P.; Quintanar, L.; Griesinger, C.; Fernández, C. O., *Inorg. Chem.* **2010**, *49*, 10668.
40. Bortolus, M.; Bisaglia, M.; Zoleo, A.; Fittipaldi, M.; Benfatto, M.; Bubacco, L.; Maniero, A. L., *J. Am. Chem. Soc.* **2010**, *132*, 18057.
41. Drew, S. C.; Leong, S. L.; Pham, C. L.; Tew, D. J.; Masters, C. L.; Miles, L. A.; Cappai, R.; Barnham, K. J., *J. Am. Chem. Soc.* **2008**, *130*, 7766.
42. Dudzik, C. G.; Walter, E. D.; Millhauser, G. L., *Biochemistry* **2011**, *50*, 1771.
43. Jackson, M. S.; Lee, J. C., *Inorg. Chem.* **2009**, *48*, 9303.
44. Kowalik-Jankowska, T.; Rajewska, A.; Jankowska, E.; Grzonka, Z., *Dalton Trans.* **2006**, *2006*, 5068.
45. Kowalik-Jankowska, T.; Rajewska, A.; Wiśniewska, K.; Grzonka, Z.; Jezierska, J., *J. Inorg. Biochem.* **2005**, *99*, 2282.
46. Lee, J. C.; Gray, H. B.; Winkler, J. R., *J. Am. Chem. Soc.* **2008**, *130*, 6898.
47. Sung, Y. H.; Rospigliosi, C.; Eliezer, D., *Biochim. Biophys. Acta* **2006**, *1561*, 5.
48. Valensin, D.; Camponeschi, F.; Luczkowski, M.; Baratto, M. C.; Remelli, M.; Valensin, G.; Kozłowski, H., *Metallomics* **2011**, *3*, 292.
49. Sóvágó, I.; Kállay, C.; Várnagy, K., *Coord. Chem. Rev.* **2012**, *256*, 2225.
50. Sigel, H.; Martin, R. B., *Chem. Rev.* **1982**, *82*, 385.
51. Drew, S. C.; Barnham, K. J., *Acc. Chem. Res.* **2011**, *44*, 1146.
52. Hureau, C.; Dorlet, P., *Coord. Chem. Rev.* **2012**, *256*, 2175.
53. Buell, A. K.; Galvagnion, C.; Gaspar, R.; Sparr, E.; Vendruscolo, M.; Knowles, T. P. J.; Linse, S.; Dobson, C. M., *Proc. Natl. Acad. Sci. U. S. A.* **2014**, *111*, 7671.
54. Lee, H.-L.; Bae, E.-J.; Lee, S.-J., *Nature Review Neurology* **2014**, *10*, 92.
55. Williams-Smith, D. L.; Bray, R. C.; Barber, M. J.; Tsopanakis, A. D.; Vincent, S. P., *Biochemistry Journal* **1977**, *167*, 593.
56. Davies, P.; Wang, X.; Sarell, C. J.; Drewett, A.; Marken, F.; Viles, J. H.; Brown, D. R., *Biochemistry* **2011**, *50*, 37.
57. Stoll, S.; Schweiger, A., *J. Magn. Reson.* **2006**, *178*, 42.

Deciphering the exact mode of copper(II) binding to α S is important in the Parkinson Disease context. In the scenario proposed here, the remote His at position 50 plays the role of a pH and copper(II) concentration dependent molecular switch between three possible copper(II) binding sites. It is anticipated that the way His binds to the copper(II) ion can induce different folding of the α S protein leading to various aggregation propensity.

